ACS Medicinal Chemistry Letters

pubs.acs.org/acsmedchemlett Letter

Stepwise Nitric Oxide Release and Antibacterial Activity of a Nitric Oxide Photodonor Hosted within Cyclodextrin Branched Polymer Nanocarriers

Tassia J. Martins,[†] Cristina Parisi,[†] Juliana Guerra Pinto, Isabelle de Paula Ribeiro Brambilla, Milo Malanga, Juliana Ferreira-Strixino, and Salvatore Sortino*

Cite This: ACS Med. Chem. Lett. 2024, 15, 857−863 Read Online

ACCESS | Metrics & More | Article Recommendations | Supporting Information

ABSTRACT: A hydrophobic nitric oxide (NO) photodonor integrating both nitroso and nitro functionalities within its chromophoric skeleton has been synthesized. Excitation of this compound with blue light triggers the release of two NO molecules from the nitroso and the nitro functionalities via a stepwise mechanism. Encapsulation of the NO photodonor within biocompatible neutral, cationic, and anionic β-cyclodextrin branched polymers as suitable carriers leads to supramolecular nanoassemblies, which exhibit the same nature of the photochemical processes but NO photorelease performances enhanced by about 1 order of magnitude when compared with the free guest. Antibacterial tests carried out with methicillin-resistant *Staphylococcus aureus* and *Acinetobacter baumannii* demonstrate an effective antibacterial activity exclusively under light activation and point out a differentiated role of the polymeric nanocarriers in determining the outcome of the antibacterial photodynamic action.

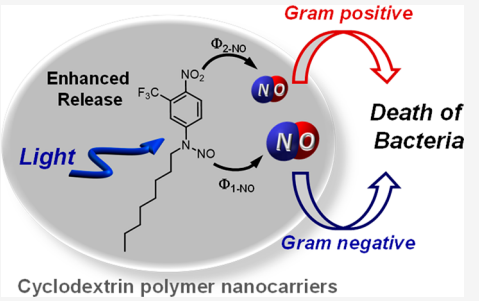

KEYWORDS: *Light, Nitric oxide, Cyclodextrin polymers, Antibacterial*

The recognition that nitric oxide (NO) plays multiple roles in physiology and pathophysiology[1] has led to the exciting prospect of exploiting this inorganic free radical as an "unconventional" drug in the treatment of severe diseases,[2,3] including bacterial infection,[4] neurodegeneration,[5] and cancer.[6] The difficulties in handling gaseous NO have pushed the research over the past two decades toward the development of an arsenal of NO-releasing precursors, integrated within tailored molecular or macromolecular skeletons and nanomaterials, that can store NO and then release this radical, in most cases spontaneously.[7−12] The strict dependence of the therapeutic effects of NO on its doses and site of action[13,14] makes the spatiotemporally controlled NO release highly desirable. This critical need has made NO precursors activatable by light stimuli, usually named NO photodonors (NOPDs), very appealing, given the unique advantage light-triggering offers in controlling the delivery process in both space and time with high precision.[15−20]

Due to the slow creation of new clinically approved antibiotic drugs and the inevitable problem of multidrug resistance (MDR),[21] the search for novel antibacterial treatment modalities represents one of the main challenges in biomedicine.[22] NO represents a promising alternative to conventional antibiotic drugs, given the combination of unique properties such as (i) absence of MDR,[23] (ii) multitarget activity,[24] (iii) broad spectrum of action,[25] and (iv) confinement of its cytotoxic action over distance <200 μm from its generation site, as a result of its short half-life (ca. 1 s).[1]

Delivering NOPDs through suitable nanocarrier systems is of relevance for multiple reasons.[26] Host nanocarriers can, in fact, (i) increase the solubility of poorly water-soluble NOPDs, (ii) play an active role as reactants due to microenvironment effects, (iii) concentrate a large number of molecules in a very small volume, increasing the light-harvesting properties and producing a highly localized "burst" of NO precisely at the desired site, and finally, (iv) encourage specific interactions with the bacterial membranes.

In this frame, cyclodextrin (CD) branched polymers (poly-CDs) represent an intriguing class of nanocarriers. They are made of CD units (α, β, or γ) cross-linked though the epichlorohydrin cross-linker agent and are well soluble in water, are bioeliminable, and exhibit good tolerance both *in vitro* and *in vivo*.[27−29] Poly-CDs have proven to be excellent host systems for the complexation, stabilization, and solubilization of a wide range of therapeutic and photo-therapeutic guest compounds with larger binding constants and payloads as compared with the unmodified CDs, due to

Received: February 3, 2024
Revised: April 16, 2024
Accepted: April 28, 2024
Published: May 9, 2024

Scheme 1. Molecular Structure of NOPD1 and the Poly-βCDs Used as Host Nanocarriers; Inset: Stepwise Mechanism for the NO Photorelease

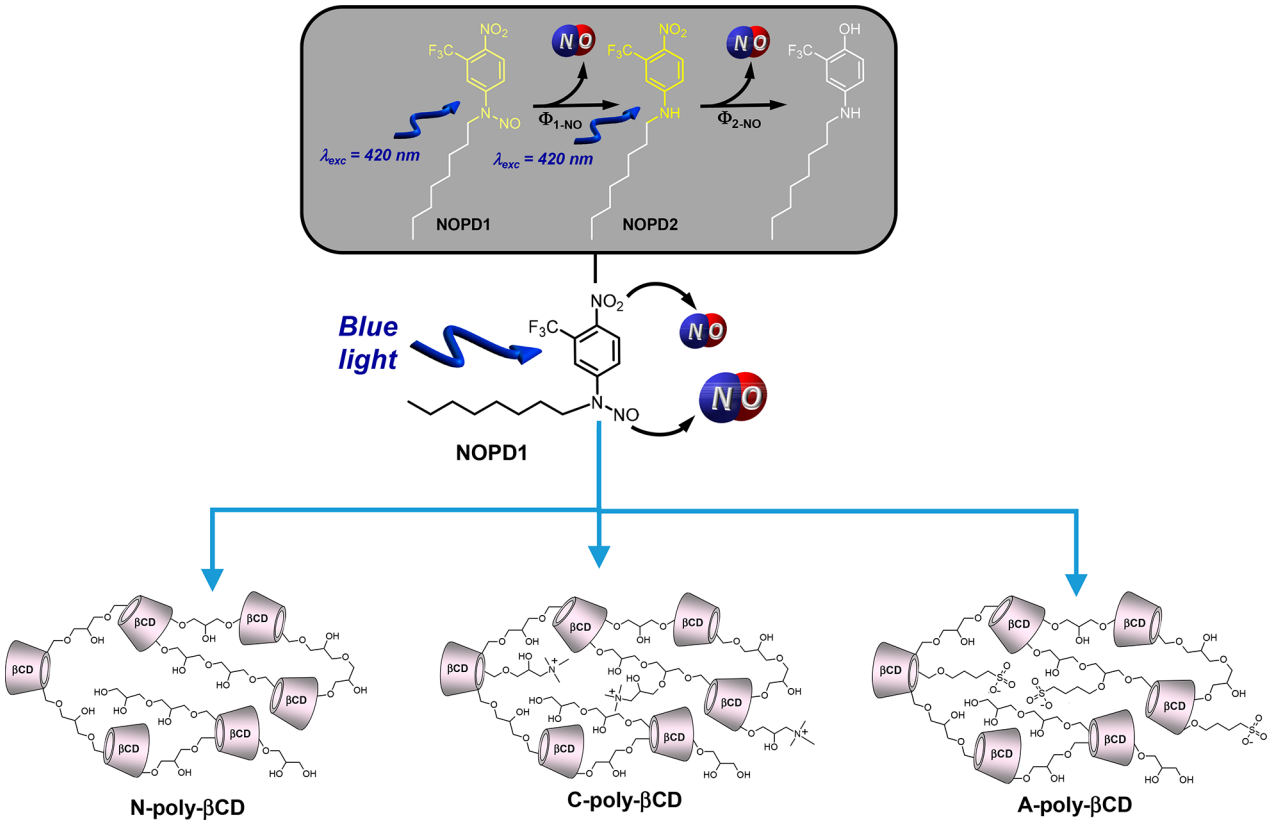

the presence of nanodomains with different and specific features.[30−34]

With the goal of achieving an NOPD able to release multiple NO molecules, herein we have devised the hydrophobic **NOPD1** (Scheme 1). It is based on the 4-nitro-3-(trifluoromethyl)aniline scaffold, an NOPD developed and extensively used in our group,[32−35] tailored with an apolar alkyl chain and a nitroso functionality. We show that blue light excitation of this compound leads to NO photorelease from the nitroso and nitro functionalities through the stepwise mechanism illustrated in Scheme 1. The highly hydrophobic **NOPD1** effectively encapsulates within the water-soluble neutral (**N-poly-βCD**), cationic (**C-poly-βCD**), and anionic (**A-poly-βCD**) poly-CDs (Scheme 1). We demonstrate that all the polymer nanocarriers do not alter the nature of the primary photochemical reactions but enhance the efficiency of NO photogeneration in both NO photorelease steps by about 1 order of magnitude and to a similar extent. Antibacterial tests performed with methicillin-resistant *Staphylococcus aureus* (MRSA) and *Acinetobacter baumannii* show differentiated antibacterial action, highlighting the key role the type of poly-βCD nanocarrier plays in determining the outcome of the antibacterial photodynamic action.

The synthetic steps involved in the preparation of **NOPD1** are reported in Scheme 2, and they are described in detail in the Supporting Information. All operations were carried out under a low-intensity level of visible light. Briefly, the direct coupling of commercial octylamine with 5-fluoro-2-nitrobenzotrifluoride in acetonitrile at room temperature gave rise to **NOPD2**, which in turn yielded nitroso derivative **NOPD1** through nitrosation with $NaNO_2$ and CH_3COOH.

Scheme 2[a]

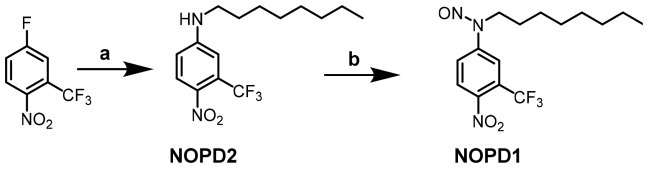

[a]Reagents and conditions: **a**) octylamine, K_2CO_3, CH_3CN, r.t., 24 h; **b**) **NOPD2**, $NaNO_2$, THF/CH_3COOH 2:1, 12 h, 0 °C → r.t.

Figure 1 shows the absorption spectrum of **NOPD1** and, for comparison, that of the non-nitrosated analogue **NOPD2** in a PBS:MeOH mixture. Both compounds exhibit similar molar

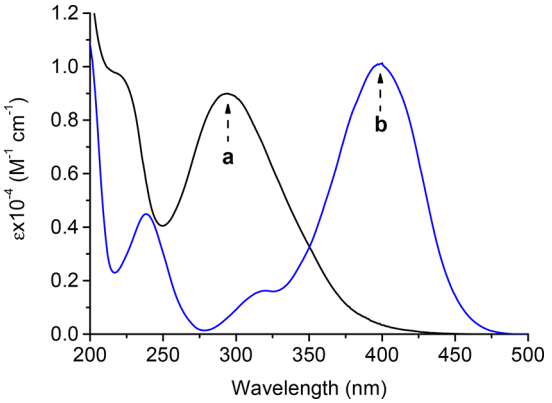

Figure 1. Absorption spectra of **NOPD1** (**a**) and **NOPD2** (**b**). PBS (10 mM; pH 7.4):MeOH 1:1 v/v; T = 25 °C.

https://doi.org/10.1021/acsmedchemlett.4c00061
ACS Med. Chem. Lett. 2024, 15, 857−863

absorptivity, but the absorption maximum of **NOPD1** is almost 100 nm blue-shifted due to the loss of the push−pull character of the nitroaniline chromophore after nitrosation. Photolysis experiments were then carried out under visible light at λ_{exc} = 420 nm. Despite the very low absorption of **NOPD1** at this excitation wavelength, the compound is responsive to light stimuli.

The photolysis profile is biphasic. The first step (Figure 2A) shows bleaching of the main absorption UV band at 290 nm,

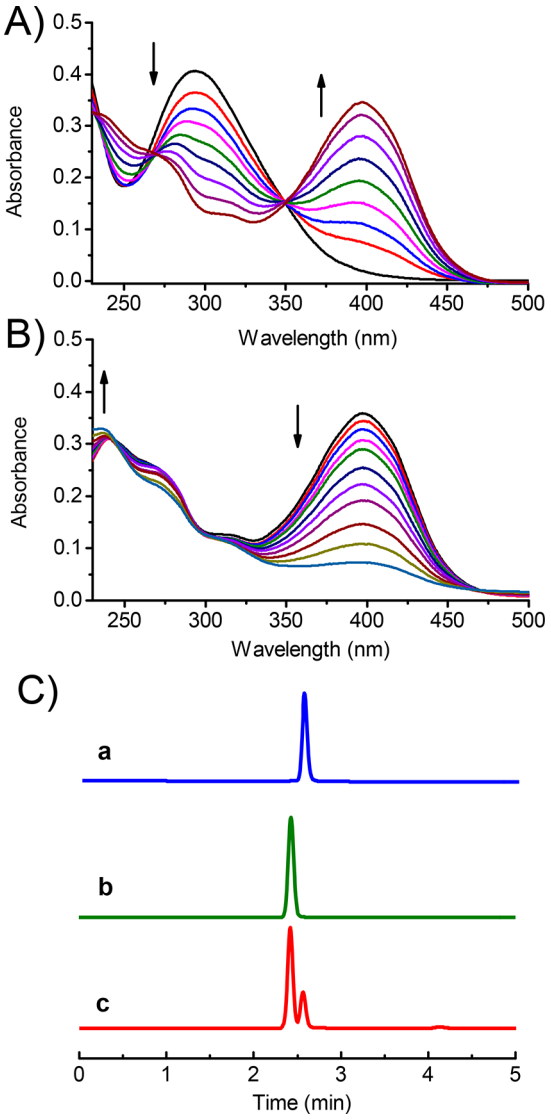

Figure 2. Absorption spectral changes observed upon exposure of an air-equilibrated solution of **NOPD1** (45 μM) at λ_{exc} = 420 nm at different irradiation times from 0 to 40 min (A) and from 40 to 100 min (B). The arrows indicate the course of the spectral profile with illumination time (C). HPLC traces related to solutions of **NOPD1** (**a**), the authentic photoproduct **NOPD2** used as a reference (**b**), and **NOPD1** after 30 min irradiation (**c**). PBS (10 mM; pH 7.4):MeOH 1:1 v/v; T = 25 °C.

accompanied by the formation of a new and intense absorption band in the visible region with a maximum at 400 nm. The second step (Figure 2B) is characterized by bleaching of the new band at 400 nm. The photochemical profiles of both steps are characterized by the presence of clear isosbestic points, which are indicative of clean photochemical processes. The band at 400 nm generated during the first photolytic step is basically the same as that of the non-nitrosated **NOPD2** (see spectrum **b** in Figure 1 for comparison). Formation of this compound as the sole stable photoproduct in the initial part of the photolysis was well confirmed by HPLC analysis carried out with the authentic **NOPD2** sample and the irradiated mixture (Figure 2C) and accounts for the loss of NO from the nitroso moiety triggered by the homolytic rupture of the N−NO bond, typical for *N*-nitrosoaniline moieties.[36−41]

As far as the second photolytic step is concerned, the spectral profile reported in Figure 2B closely resembles that typically observed for the irradiation of several derivatives of the 4-nitro-3-(trifluoromethyl)aniline chromophoric scaffold extensively used in our group.[32−35] In fact, NO photorelease from this unit takes place after a nitro-to-nitrite photorearrangement, leading to phenol derivatives absorbing in the UV region and being responsible for the photobleaching observed. Overall, these findings account for the generation of two NO molecules through the stepwise mechanism illustrated in Scheme 1. The quantum yields related to the two sequential processes were calculated to be $\Phi_{1\text{-NO}} = 4.3 \times 10^{-3}$ and $\Phi_{2\text{-NO}} = 0.7 \times 10^{-3}$, respectively. Note that the larger absorption coefficient of **NOPD2** at the excitation wavelength compensates for the smaller value of $\Phi_{2\text{-NO}}$.

The neutral, cationic, and anionic poly-βCDs, **N-poly-βCD**, **C-poly-βCD**, and **A-poly-βCD**, respectively, sketched in Scheme 1 were used as carrier systems. All these polymers are well soluble in aqueous medium and suitable to encapsulate highly hydrophobic guests.[30−34,42,43] **NOPD1** and its phototoproduct **NOPD2** are not soluble in aqueous solution. However, both compounds become fairly soluble in the presence of the polymeric hosts, as indicated by the appearance of their characteristic absorption bands at ca. 290 and 400 nm, respectively (Figure 3).

Note that both the band profiles and the absorption maxima of the guests exhibit only slight differences for all three hosts and are very similar to those observed for the free guests in PBS:MeOH solution (see Figure 1 for comparison). This suggests a quite similar polarity environment experienced by the two guests within the polymeric hosts and rules out significant inter-chromophoric interactions therein. Table 1 reports the apparent solubility (S_a) and the hydrodynamic diameter (D_H), and Table S1 (SI) reports the encapsulation efficiency and loading capacity for all of the host−guest NOPD/poly-βCD assemblies. They were quite stable in the dark at room temperature for at least 48 h, as confirmed by the negligible variation of the absorbances observed over this time window.

Photolysis experiments were then carried out in PBS aqueous solution. Figure 4A,B shows representative results obtained in the case of **NOPD1/C-poly-βCD**.

The photolysis profile shows the initial formation of the typical band of **NOPD2** at ca. 400 nm, followed by its bleaching for longer irradiation times. A very similar photobehavior was observed for the **NOPD1/N-poly-βCD** and **NOPD1/A-poly-βCD** nanoassemblies (Figures S9 and S10 (SI)). Figure 4C reports the absorbance evolution monitored at 400 nm as a function of the irradiation time in the case of the three supramolecular nanoassemblies from which a typical biphasic photobehavior can be noted. These findings parallel those observed for the free guest and suggest that the polymeric hosts do not alter the nature of the primary photochemical processes of **NOPD1** after encapsulation.

https://doi.org/10.1021/acsmedchemlett.4c00061
ACS Med. Chem. Lett. 2024, 15, 857−863

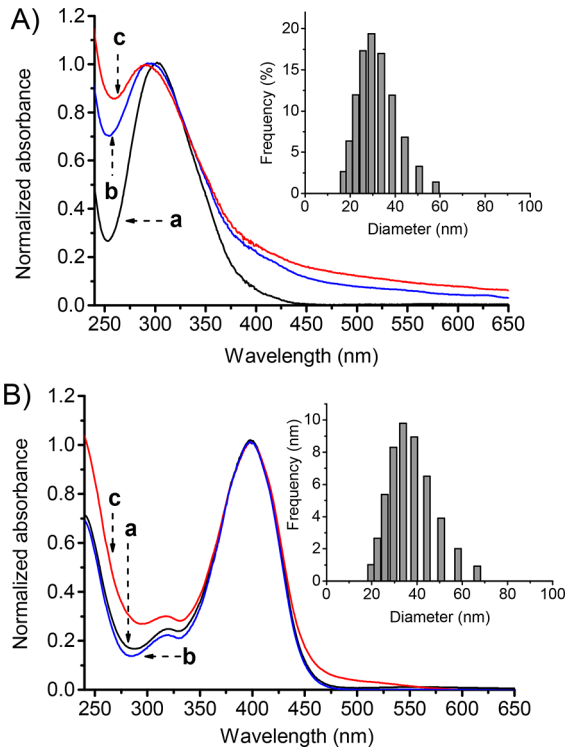

Figure 3. Normalized absorption spectra of **NOPD1** (A) and **NOPD2** (B) in the presence of aqueous dispersions (4 mg mL^{-1}) of **N-poly-βCD** (**a**), **C-poly-βCD** (**b**), and **A-poly-βCD** (**c**). The insets show representative hydrodynamic diameters in the case of nanoassemblies **NOPD1/N-poly-βCD** (A) and **NOPD2/N-poly-βCD** (B). PBS (10 mM; pH 7.4); T = 25 °C.

Table 1. Properties of the Poly-βCD Assemblies with NOPD1 and NOPD2[a]

Sample	S_a (μg mL^{-1})	D_H (nm)
NOPD1/N-poly-βCD	4.3 ± 0.3	21.4 ± 0.5
NOPD1/C-poly-βCD	4.3 ± 0.3	15.5 ± 0.8
NOPD1/A-poly-βCD	2.4 ± 0.2	23.4 ± 0.6
NOPD2/N-poly-βCD	15.8 ± 1.1	18.8 ± 0.9
NOPD2/C-poly-βCD	11.7 ± 0.9	14.5 ± 0.5
NOPD2/A-poly-βCD	11.5 ± 1.0	20.2 ± 0.8

[a]Results are reported as the mean of three separate measurements on three different batches ± SD.

However, as shown in Table 2, the quantum yields related to the first and second reaction steps were both ca. 1 order of magnitude larger than that observed for the free **NOPD1**. Moreover, the values obtained were comparable for all of the nanoassemblies. This enhanced photoreactivity in the polymers is not uncommon for free-radical-mediated photodecomposition pathways, such as those leading to NO release. In fact, it may be the result of the active role the polymeric network of the hosts plays in providing easily abstractable hydrogens close to the anilinyl radical intermediate involved in the mechanism of the NO photorelease[41] in the case of **NOPD1** and the phenoxyl intermediate generated after NO photorelease from **NOPD2**.[32,34] Finally, the similar values for $\Phi_{1\text{-NO}}$ and $\Phi_{2\text{-NO}}$ observed for all hosts suggest that their different charges do not affect the primary photodecomposition processes.

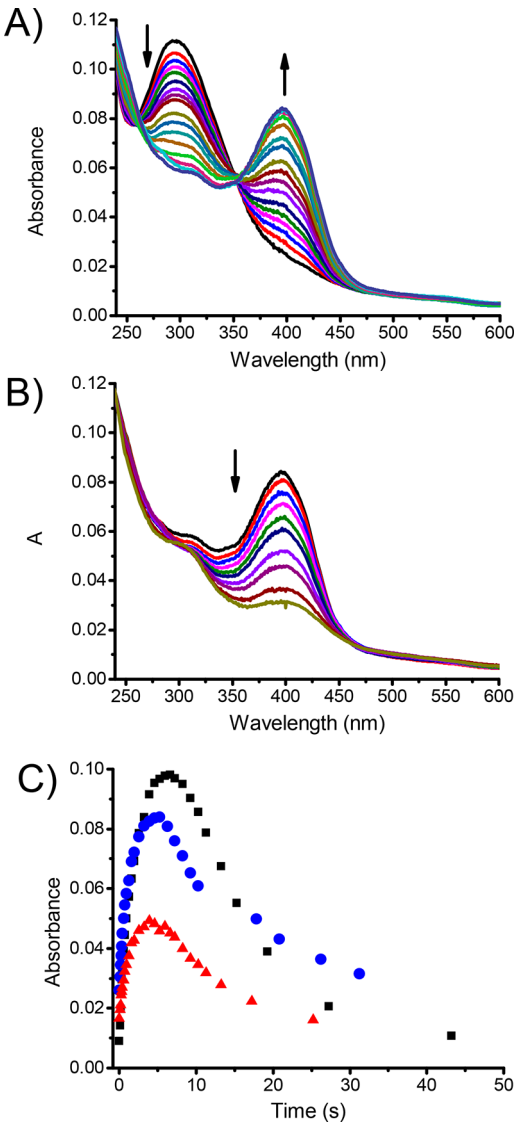

Figure 4. Absorption spectral changes observed upon exposure of an air-equilibrated aqueous suspension of **NOPD1/C-poly-βCD** at λ_{exc} = 420 nm at different irradiation times from 0 to 5 min (A) and from 5 to 31 min (B). The arrows indicate the course of the spectral profile with the illumination time. (C) Evolution of the absorbance at 400 nm upon irradiation at λ_{exc} = 420 nm of air-equilibrated aqueous suspensions of **NOPD1/N-poly-βCD** (■), **NOPD1/C-poly-βCD** (●), and **NOPD1/A-poly-βCD** (▲). **NOPD1/N-poly-βCD** ([**NOPD1**] = 12 μM); **NOPD1/C-poly-βCD** ([**NOPD1**] = 10 μM); **NOPD1/A-poly-βCD** ([**NOPD1**] = 7 μM); [**N-poly-βCD**] = [**C-poly-βCD**] = [**A-poly-βCD**] = 4 mg mL^{-1}. PBS (10 mM; pH 7.4); T = 25 °C.

Table 2. Quantum Yields Related to the First and Second Photolysis Steps (T = 25 °C)

Sample	$\Phi_{1\text{-NO}}$	$\Phi_{2\text{-NO}}$
NOPD1[a]	4.3×10^{-3}	0.7×10^{-3}
NOPD1/N-poly-βCD	4.8×10^{-2}	5.5×10^{-3}
NOPD1/C-poly-βCD	4.9×10^{-2}	4.8×10^{-3}
NOPD2/A-poly-βCD	4.3×10^{-2}	5.0×10^{-3}

[a]Dissolved in PBS (10 mM; pH 7.4):MeOH 1:1.

Direct evidence for the stepwise release of NO was unambiguously provided by detecting this radical through an

https://doi.org/10.1021/acsmedchemlett.4c00061
ACS Med. Chem. Lett. 2024, 15, 857−863

amperometric technique using an ultrasensitive NO electrode. Figure 5 shows that all nanoassemblies of **NOPD1** and its

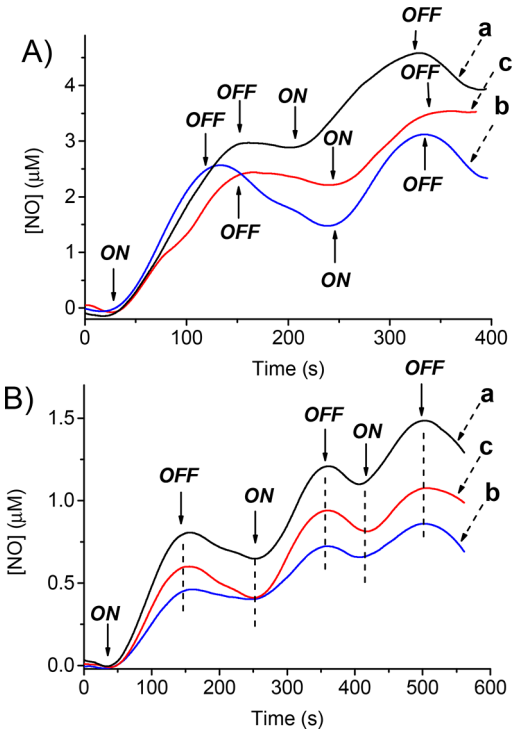

Figure 5. NO release profiles observed upon alternate ON/OFF cycles of irradiation at λ_{exc} = 405 nm for aqueous suspensions of (A) **NOPD1/N-poly-βCD** (**a**), **NOPD1/C-poly-βCD** (**b**), and **NOPD1/A-poly-βCD** (**c**) and (B) **NOPD2/N-poly-βCD** (**a**), **NOPD2/C-poly-βCD** (**b**), and **NOPD2/A-poly-βCD** (**c**). [**NOPD1**] = [**NOPD2**] = 8 μM; [**N-poly-βCD**] = [**C-poly-βCD**] = [**A-poly-βCD**] = 4 mg mL^{-1}. PBS (10 mM; pH 7.4); T = 25 °C.

authentic stable photoproduct **NOPD2** formed after the first photolytic step release NO under light input. The NO release stops in the dark and restarts once the illumination is turned on again. Note that the efficiency values for the NO photorelease from the nanoassemblies of **NOPD1** were very similar to each other, as were those for the nanoassemblies of **NOPD2**. These results are in agreement with the similar quantum yields related to the first and second photolytic steps, respectively, observed for the three supramolecular nanoassemblies.

Antibacterial activity of the nanoassemblies and, for comparison, the free **NOPD1** were tested on methicillin-resistant *Staphylococcus aureus* (MRSA) and *Acinetobacter baumannii*. These are specimens of Gram-positive and Gram-negative bacteria responsible for higher rates of morbidity due to the high antibiotic resistance pattern toward traditional antibiotics. Figure 6 reports the results obtained for the bacterial cultures either kept in the dark or irradiated for 10 min with a blue LED. Based on the light intensity used, both NO photorelease steps are expected to occur under these experimental conditions. It can be seen that free **NOPD1** did not show any significant antibacterial action against either bacterial strain, neither in the dark nor upon irradiation. Besides, all the polymeric nanoassemblies did not inhibit the growth of both bacterial strains in the dark. In contrast, in the case of MRSA, total inhibition was observed for **NOPD1** delivered through the anionic nanocarrier **A-poly-βCD**. A

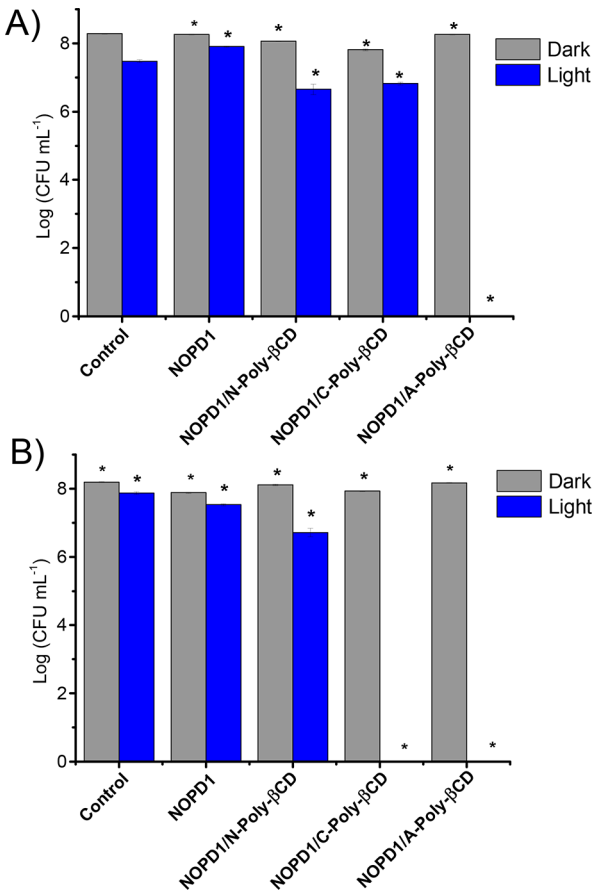

Figure 6. Planktonic assay for (A) MRSA and (B) *A. baumannii* (1×10^8 CFU mL^{-1}) incubated with the free **NOPD1** (1% DMSO) and its nanoassemblies with poly-βCD, suspended in PBS (10 mM; pH 7.4) and either kept in the dark or irradiated with blue light at λ_{exc} = 420 nm (ca. 96 mW cm^{-2}). Untreated bacteria were used as a control. Statistical analyses via One Way Anova and Tukey tests indicate a statistically significant difference (*$p < 0.01$). [**NOPD1**] = 10 μM; [**N-poly-βCD**] = [**C-poly-βCD**] = [**A-poly-βCD**] = 4 mg mL^{-1}.

photodynamic effect, but to a much lesser extent, with a Log reduction of the initial bacterial burden ca. 2, was also observed for the nanoassembly with **N-poly-βCD** and **C-poly-βCD**. In the case of *A. baumannii*, nanoassemblies of both anionic and cationic polymeric nanocarriers showed a remarkable photodynamic action, leading to a total inhibition of the bacteria growth. Additionally, a Log reduction of the initial bacterial burden of ca. 2 was observed for **NOPD1** delivered through neutral **N-poly-βCD**. Note that the bactericidal action on MRSA is relevant because of the distinctive ability of this pathogen to withstand high endogenous NO concentrations by expressing flavohemoglobin in concert with inducible homolactic fermentation, which serves to maintain redox balance during nitrosative stress.[44] *A. baumannii* has become an essential agent in hospital-acquired infections related to ventilator-associated pneumonia with a high mortality rate. Additionally, it is associated with burn infections and central nervous system infections. MDR reduces the treatment possibilities used clinically.[45,46] Furthermore, both *S. aureus* and *A. baumannii* are on the list of emerging bacteria of medical importance due to bacterial resistance. They are classified in the group of essential pathogens known as ESCAPE (*Enterococcus faecium*, *Staphylococcus aureus*, *Clostridium difficile*, *Acinetobacter* species, *P. aeruginosa*, and *Enter-*

https://doi.org/10.1021/acsmedchemlett.4c00061
ACS Med. Chem. Lett. 2024, 15, 857−863

obacteriaceae).[47] The ability to reduce the viability of two important bacteria from this group is therefore a significant result.

A key point that needs to be highlighted is that the antibacterial activity exhibited by the nanoassemblies upon light irradiation cannot be simply attributed to the enhancement of the NO photorelease efficiency of encapsulated **NOPD1**. In fact, the nanoassemblies exhibited different photodynamic actions despite, as reported in Table 2, showing comparable quantum yields for the sequential NO release processes. Therefore, this finding points out a different role for each nanocarrier in the delivery process of **NOPD1** for different bacterial strains, probably controlled through specific interactions with bacterial membranes.

In conclusion, we have reported a hydrophobic NO donor that releases two NO molecules upon blue light irradiation through a stepwise process. This NO photoreleaser can be entrapped with similar efficiency within neutral, cationic, and anionic branched poly-CD, leading to nanoassemblies having comparable sizes. The nature of the stepwise NO release process is preserved upon guest encapsulation in the polymeric hosts, but the efficiency of both photolytic steps is enhanced by about 1 order of magnitude. Antibacterial tests performed with the Gram-positive MRSA and the Gram-negative *A. baumannii* show a total growth inhibition of the former by the negatively charged nanoassembly and of the latter by both the negatively and positively charged nanoassemblies. The very similar quantum efficiencies for the NO photogeneration observed in all nanoassemblies, combined with their differentiated antibacterial activity, suggest that, in addition to enhancing the efficiency of the NO photorelease, the nature of the polymeric nanocarriers plays a key role in determining the outcome of the photodynamic action. Further studies to better clarify this point are currently in progress.

■ ASSOCIATED CONTENT

Supporting Information

The Supporting Information is available free of charge at https://pubs.acs.org/doi/10.1021/acsmedchemlett.4c00061.

Synthetic and experimental procedures, antibacterial protocols, and photolysis profiles of poly-CD nanoassemblies not reported in the main text (PDF)

■ AUTHOR INFORMATION

Corresponding Author

Salvatore Sortino − *PhotoChemLab, Department of Drug Sciences, University of Catania, I-95125 Catania, Italy;* orcid.org/0000-0002-2086-1276; Email: ssortino@unict.it

Authors

Tassia J. Martins − *PhotoChemLab, Department of Drug Sciences, University of Catania, I-95125 Catania, Italy*

Cristina Parisi − *PhotoChemLab, Department of Drug Sciences, University of Catania, I-95125 Catania, Italy*

Juliana Guerra Pinto − *Laboratory of Photobiology Applied to Health, Research and Development Institute, University of Vale do Paraíba, Urbanova I-2911, Brazil*

Isabelle de Paula Ribeiro Brambilla − *Laboratory of Photobiology Applied to Health, Research and Development Institute, University of Vale do Paraíba, Urbanova I-2911, Brazil*

Milo Malanga − *CarboHyde, I-1045 Budapest, Hungary*

Juliana Ferreira-Strixino − *Laboratory of Photobiology Applied to Health, Research and Development Institute, University of Vale do Paraíba, Urbanova I-2911, Brazil*

Complete contact information is available at: https://pubs.acs.org/10.1021/acsmedchemlett.4c00061

Author Contributions

†T.J.M. and C.P. contributed equally.

Notes

The authors declare no competing financial interest.

■ ACKNOWLEDGMENTS

We thank HORIZON-MSCA-2021-PF-01, 101057562 - SUPREME for financial support to MC fellow T.J.M. and funding of the research. JGP - FAPESP - 2022/10251-0, IPRB - Coordination for the Improvement of Higher Education Personnel - Brazil (CAPES) - Finance Code 001.

■ REFERENCES

(1) Ignarro, L. J. *Nitric Oxide: Biology and Pathobiology*; Elsevier: St. Louis, 2010.

(2) Wang, Z.; Jin, A.; Yang, Z.; Huang, W. Advanced nitric oxide generating nanomedicine for therapeutic applications. *ACS Nano* **2023**, *17*, 8935−8965.

(3) Carpenter, A. W.; Schoenfisch, M.-H. Nitric oxide release: Part II. Therapeutic applications. *Chem. Soc. Rev.* **2012**, *41*, 3742−3752.

(4) Yang, L.; Feura, E. S.; Ahonen, M. J. R.; Schoenfisch, M. H. Nitric oxide-releasing macromolecular scaffolds for antibacterial applications. *Adv. Healthc. Mater.* **2018**, *7*, 1800155.

(5) Tewari, D.; Sah, A. N.; Bawari, S.; Nabavi, S. F.; Dehpour, A. R.; Shirooie, S.; Braidy, N.; Fiebich, B. L.; Vacca, R. A.; Nabavi, S. M. Role of nitric oxide in neurodegeneration: function, regulation, and inhibition. *Curr. Neuropharmacol.* **2020**, *19*, 114−126.

(6) Fukumura, D.; Kashiwagi, S.; Jain, R. K. The role of nitric oxide in tumour progression. *Nat. Rev. Cancer* **2006**, *6*, 521−534.

(7) Navale, G. R.; Singh, S.; Ghosh, K. NO donors as the wonder molecules with therapeutic potential: Recent trends and future perspectives. *Coord. Chem. Rev.* **2023**, *481*, 215052.

(8) Wang, P. G.; Xian, M.; Tang, X.; Wu, X.; Wen, Z.; Cai, T.; Janczuk, A. J. Nitric oxide donors: chemical activities and biological applications. *Chem. Rev.* **2002**, *102*, 1091−1134.

(9) Qian, Y.; Kumar, R.; Chug, M. K.; Massoumi, H.; Brisbois, E. J. Therapeutic delivery of ntric oxide utilizing saccharide-based materials. *ACS Appl. Mater. Interfaces* **2021**, *13*, 52250−52273.

(10) Wang, P. G.; Cai, T. B.; Taniguchi, N. *Nitric oxide donors*; Wiley-VCH: Weinheim, 2005.

(11) Riccio, D. A.; Schoenfisch, M. H. Nitric oxide release: Part I. Macromolecular scaffolds. *Chem. Soc. Rev.* **2012**, *41*, 3731−3741.

(12) Seabra, A. B.; Duran, N. Nitric oxide-releasing vehicles for biomedical applications. *J. Mater. Chem.* **2010**, *20*, 1624−1637.

(13) Janczuk, A. J; Jia, Q.; Xian, M.; Wen, Z.; Wang, P. G.; Cai, T. NO donors with anticancer activity. *Expert Opin. Ther. Patents.* **2002**, *12*, 819−826.

(14) Huang, Z.; Fu, J.; Zhang, Y. Nitric oxide donorbased cancer Therapy: advances and prospects. *J. Med. Chem.* **2017**, *60*, 7617−7635.

(15) Sortino, S. Light-controlled nitric oxide delivering molecular assemblies. *Chem. Soc. Rev.* **2010**, *39*, 2903−2913.

(16) Ford, P. C. Photochemical delivery of nitric oxide. *Nitric Oxide* **2013**, *34*, 56−64.

(17) Ford, P. C. Metal complex strategies for photo-uncaging the small molecule bioregulators nitric oxide and carbon monoxide. *Coord. Chem. Rev.* **2018**, *376*, 548−564.

(18) Fry, N. L.; Mascharak, P. K. Photoactive ruthenium nitrosyls as NO donors: how to sensitize them toward visible light. *Acc. Chem. Res.* **2011**, *44*, 289−298.
(19) Ieda, N.; Oka, Y.; Yoshihara, T.; Tobita, S.; Sasamori, T.; Kawaguchi, M.; Nakagawa, H. Structure-efficiency relationship of photoinduced electron transfer-triggered nitric oxide releasers. *Sci. Report* **2019**, *9*, 1430.
(20) Fraix, A.; Parisi, C.; Seggio, M.; Sortino, S. Nitric oxide photoreleasers with fluorescent reporting. *Chem.—Eur. J.* **2021**, *27*, 12714−12725.
(21) Murray, C. J.; Ikuta, K. S.; Sharara, F.; Swetschinski, L.; Aguilar, G. R.; Gray, A.; Han, C.; Bisignano, C.; Rao, P.; Wool, E.; Johnson, S. C.; et al. Global burden of bacterial antimicrobial resistance in 2019: a systematic analysis. *Lancet* **2022**, *399*, 629−655.
(22) Nwobodo, D. C.; Ugwu, M. C.; Anie, C. O.; Al-Ouqaili, M. T. S; Ikem, J. C.; Chigozie, U. V.; Saki, M. Antibiotic resistance: The challenges and some emerging strategies for tackling a global menace. *J. Clin Lab Anal.* **2022**, *36*, e24655.
(23) Gardner, P. R.; Gardner, A. M.; Martin, L. A.; Salzman, A. L. *Proc. Natl. Acad. Sci. U.S.A.* **1998**, *95*, 10378−10383.
(24) Fang, F. C. Antimicrobial reactive oxygen and nitrogen species: concepts and controversies. *Nat. Rev. Microbiol.* **2004**, *2*, 820−832.
(25) Schairer, D. O.; Chouake, J. S.; Nosanchuk, J. D.; Friedman, A. J. The potential of nitric oxide releasing therapies as antimicrobial agents. *Virulence* **2012**, *3*, 271−279.
(26) Swaminathan, S.; Garcia-Amorós, J.; Fraix, A.; Kandoth, N.; Sortino, S.; Raymo, F. M. Photoresponsive polymer nanocarriers with multifunctional cargo. *Chem. Soc. Rev.* **2014**, *43*, 4167−4178.
(27) Othman, M.; Bouchemal, K.; Couvreur, P.; Desmaële, D.; Morvan, E.; Pouget, T.; Gref, R. A comprehensive study of the spontaneous formation of nanoassemblies in water by a "lock-and-key" interaction between two associative polymers. *J. Colloid Interface Sci.* **2011**, *354*, 517−527.
(28) Battistini, E.; Gianolio, E.; Gref, R.; Couvreur, P.; Fuzerova, S.; Othman, M.; Aime, S.; Badet, B.; Durand, P. High-Relaxivity Magnetic Resonance Imaging (MRI) Contrast Agent Based on Supramolecular Assembly between a Gadolinium Chelate, a Modified Dextran, and Poly-β-Cyclodextrin. *Chem.—Eur. J.* **2008**, *14*, 4551−4561.
(29) Daoud-Mahammed, S.; Couvreur, P.; Bouchemal, K.; Cheron, M.; Lebas, G.; Amiel, C.; Gref, R. Cyclodextrin and Polysaccharide-Based Nanogels: Entrapment of Two Hydrophobic Molecules, Benzophenone and Tamoxifen. *Biomacromolecules* **2009**, *10*, 547−554.
(30) Agnes, M.; Pancani, E.; Malanga, M.; Fenyvesi, E.; Manet, I. Implementation of Water-Soluble Cyclodextrin-Based Polymers in Biomedical Applications: How Far Are We? *Macromol. Biosci.* **2022**, *22* (8), No. 2200090.
(31) Pancani, E.; Veclani, D.; Agnes, M.; Mazza, A.; Ven-turini, A.; Malanga, M.; Manet, I. Three-in-one: explora-tion of co-encapsulation of cabazitaxel, bicalutamide and chlorin e6 in new mixed cyclodextrin-crosslinked polymers. *RSC Adv.* **2023**, *13* (16), 10923−10939.
(32) Laneri, F.; Seggio, M.; Parisi, C.; Béni, S.; Fraix, A.; Malanga, M.; Sortino, S. A mixed β-γ-cyclodextrin branched polymer with multiple photo-chemotherapeutic cargos. *ACS Applied Polymer Mater.* **2023**, *5*, 7918−7926.
(33) Fraix, A.; Kirejev, V.; Malanga, M.; Fenyvesi, E.; Beni, S.; Ericson, M. B.; Sortino, S. A three-color fluorescent supramolecular nanoassembly of phototherapautics activatable by two-photon excitation with near infrared light. *Chem.—Eur. J.* **2019**, *25*, 7091−7095.
(34) Malanga, M.; Seggio, M.; Kirejev, V.; Fraix, A.; Di Bari, I.; Fenyvesi, E.; Ericson, M. B.; Sortino, S. A phototherapeutic fluorescent β-cyclodextrin branched polymer delivering nitric oxide. *Biomater. Sci.* **2019**, *7*, 2272−2276.
(35) Caruso, E. B.; Petralia, S.; Conoci, S.; Giuffrida, S.; Sortino, S. Photodelivery of Nitric Oxide from Water-Soluble Platinum Nanoparticles. *J. Am. Chem. Soc.* **2007**, *129* (3), 480−481.
(36) Ieda, N.; Hotta, Y.; Miyata, N.; Kimura, K.; Nakagawa, H. Photomanipulation of Vasodilation with a Blue-Light-Controllable Nitric Oxide Releaser. *J. Am. Chem. Soc.* **2014**, *136*, 7085−7091.
(37) Zhou, E. Y.; Knox, H.; Reinhardt, C. J.; Partipilo, G.; Nilges, M. J.; Chan, J. Near-Infrared Photoactivatable Nitric Oxide Donors with Integrated Photoacoustic Monitoring. *J. Am. Chem. Soc.* **2018**, *140*, 11686−11697.
(38) Kitamura, K.; Kawaguchi, M.; Ieda, N.; Miyata, N.; Nakagawa, H. Visible Light-Controlled Nitric Oxide Release from Hindered Nitrobenzene Derivatives for Specific Modulation of Mitochondrial Dynamics. *ACS Chem. Biol.* **2016**, *11*, 1271−1278.
(39) He, H.; Xia, Y.; Qi, Y.; Wang, H.-Y.; Wang, Z.; Bao, J.; Zhang, Z.; Wu, F.-G.; Wang, H.; Chen, D.; Yang, D.; Liang, X.; Chen, J.; Zhou, S.; Liang, X.; Qian, X.; Yang, Y. A Water-Soluble, Green-Light Triggered, and Photo-Calibrated Nitric Oxide Donor for Biological Applications. *Bioconjugate Chem.* **2018**, *29*, 1194−1198.
(40) He, H.; Ye, Z.; Xiao, Y.; Yang, W.; Qian, X.; Yang, Y. Photocalibrated NO Release from N-Nitrosated Napthalimides upon One-Photon or Two-Photon Irradiation. *Anal. Chem.* **2018**, *90*, 2164−2169.
(41) Parisi, C.; Seggio, M.; Fraix, A.; Sortino, S. A High-Performing Metal-Free Photoactivatable Nitric Oxide Donor with a Green Fluorescent Reporter. *ChemPhotoChem.* **2020**, *4*, 742−748.
(42) Akkın, S.; Varan, G.; Isık, A.; Göksen, S.; Karakoç, E.; Malanga, M.; Esendagli, G.; Korkusuz, P.; Bilensoy, E. Synergistic Antitumor Potency of a Self-Assembling Cyclodextrin Nanoplex for the Co-Delivery of 5-Fluorouracil and Interleukin-2 in the Treatment of Colorectal Cancer. *Pharmaceutics* **2023**, *15*, 314.
(43) Wankar, J.; Bonvicini, F.; Benkovics, G.; Marassi, V.; Malanga, M.; Fenyvesi, E.; Gentilomi, G. A.; Reschiglian, P.; Roda, B.; Manet, I. Widening the Therapeutic Perspectives of Clofazimine by Its Loading in Sulfobutylether β-Cyclodextrin Nanocarriers: Nanomolar IC_{50} Values against MDR S. epidermidis. *Mol. Pharmaceutics* **2018**, *15*, 3823−3836.
(44) Lewis, A. M.; Matzdorf, S. S.; Endres, J. L.; Windham, I. H.; Bayles, K. W.; Rice, K. C. Examination of the Staphylococcus aureus nitric oxide reductase (saNOR) reveals its contribution to modulating intracellular NO levels and cellular respiration. *Mol. Microbiol.* **2015**, *96*, 651−669.
(45) Dehbanipour, R.; Ghalavand, Z. Acinetobacter baumannii: Pathogenesis, virulence factors, novel therapeutic options and mechanisms of resistance to antimicrobial agents with emphasis on tigecycline. *J. Clin. Pharm. Ther.* **2022**, *47*, 1875−1884.
(46) Ibrahim, S.; Al-Saryi, N.; Al-Kadmy, I. M. S.; Aziz, S. N. Multidrug-resistant Acinetobacter baumannii as an emerging concern in hospitals. *Mol. Biol. Rep.* **2021**, *48*, 6987−6998.
(47) De Oliveira, D.; Forde, B. M.; Kidd, T. J.; Harris, P. N. A.; Schembri, M. A.; Beatson, S. A.; Paterson, D. L.; Walker, M. J. Antimicrobial Resistance in ESKAPE Pathogens. *Clin. Microbiol. Rev.* **2020**, *33*, 1−49.

https://doi.org/10.1021/acsmedchemlett.4c00061
ACS Med. Chem. Lett. 2024, 15, 857−863